Mechanism of stabilization and magnetization of impurity-doped zigzag graphene nanoribbons

Yuuki Uchida, Shun-ichi Gomi, Haruyuki Matsuyama, Akira Akaishi (iD), and Jun Nakamura

View Online   Export Citation   CrossMark

ARTICLES YOU MAY BE INTERESTED IN

2017 Journal
Impact Factor:
12.894

Applied Physics Reviews
Now accepting original research

AIP Publishing

Mechanism of stabilization and magnetization of impurity-doped zigzag graphene nanoribbons

Yuuki Uchida,[1,2] Shun-ichi Gomi,[1,2] Haruyuki Matsuyama,[1,2] Akira Akaishi,[1,2,a]
and Jun Nakamura[1,2,b]

[1]*Department of Engineering Science, The University of Electro-Communications (UEC-Tokyo),*
1-5-1 Chofugaoka, Chofu, Tokyo 182-8585, Japan
[2]*CREST, Japan Science and Technology Agency, 4-1-8 Honcho, Kawaguchi, Saitama 332-0012, Japan*

Doping is an efficient way to modify the electronic structure of graphene. Although there have been a considerable number of studies on the electronic structure of impurity-doped graphene, every study has suggested a different interpretation of the appearance of impurity levels of dopants located near the so-called zigzag edge of graphene nanoribbons (GNRs). Here, we propose a charge transfer model that satisfactorily explains the change in electronic structure upon N(B) doping of zigzag GNR (ZGNR). The structural stability and electronic structure of the doped ZGNR have been investigated using first-principles calculations based on the density functional theory. The formation energy of doping increases as a function of the distance between the N(B) atom and the zigzag edge, and two tendencies are observed depending on whether the dopant is an odd or even number of sites away from the zigzag edge. Such peculiar behavior of the formation energy can be successfully explained by charge transfer between the so-called edge state localized at the edge and the $2p$-state of the dopant. Such an electron (hole) transfer leads to the compensation (disappearance) of the local spin-magnetic moment at one side of the ZGNR, manifesting in the ferromagnetic ground state of ZGNR. *Published by AIP Publishing.* [http://dx.doi.org/10.1063/1.4971175]

I. INTRODUCTION

Graphene, a two-dimensional (2D) sheet of sp^2-bonded carbon atoms in a honeycomb arrangement, has attracted much attention as one of the promising candidates for future nanoelectronic materials owing to its exceptional electronic[1,2] and thermal[3–5] properties. Graphene nanoribbon (GNR), a one-dimensional (1D) form of graphene, has also received extensive attention because of its remarkable structural and electronic properties.[6,7] In particular, GNR with a zigzag edge, zigzag GNR (ZGNR), has an antiferromagnetic ground state, which originates from spin polarization effects in the electronic states localized at the ribbon edge, the so-called edge states.[6–12] Thus, over the past decade, numerous attempts have been made to demonstrate the utility of GNRs as magnetic materials[13,14] and in spintronic devices.[9,15,16]

To realize the graphene-based electronics or spintronics, it is important to modulate the electronic properties of GNR. The most common approach to modulate the electronic properties of GNRs is doping with heteroatoms,[17,18] as well as chemical modification of graphene edges.[19–21] For example, it has been experimentally shown that N-doped graphene exhibits n-type behavior,[22–25] whereas B-doped graphene exhibits p-type behavior.[26,27] A theoretical calculation has shown that the pyridinic N acts as an acceptor in graphene.[28] N-doped graphene has been reported to show superb performance for the oxygen reduction reaction associated with alkaline fuel cells.[29–31] Doped graphene can be synthesized using various experimental techniques. N atoms can be

doped into graphene using chemical vapor deposition (CVD),[22,25,30,32] NH_3 annealing after ion-beam irradiation,[23] or NH_3 plasma exposure.[24] B-doped graphene can also be obtained using CVD[26] or by reaction with the ionic atmosphere of trimethylboron decomposed by microwave plasma.[27] The atomic and electronic structures of such doped graphene have been characterized using scanning tunneling microscopy[25,26] and X-ray photoelectron spectroscopy.[22–27,30] Although a large number of studies have focused on experimental determination of the location of dopants, little is known about the relationship between the microscopic structure and the properties of doped graphene.

Specific properties of doped graphene are strongly dependent on the microscopic location of the dopants. The theoretical studies on the electronic structure of doped graphene have been previously reported.[33–37] It has been reported that distinct electronic states of localized π states are found to appear in the occupied and unoccupied regions near the Fermi level at the carbon atoms around pyridinic N and graphitic N species, respectively.[36] This means that the pyridinic N and graphitic N in the graphene plane are negatively and positively charged, respectively. It has also been shown that the interaction energies between two graphitic N atoms in graphene generally decrease with increasing separation distance and that two N dopants at third or seventh nearest-neighbor distance have very small interaction energies.[34,35,37] In our previous study, we investigated the dependence of the concentration of N atoms on the structural stability of homogeneously arranged N-doped graphene, and found that the formation energy of N doping increases in proportion to the density of N atoms and that anomalous

a)Electronic mail: akaishi@natori.ee.uec.ac.jp
b)Electronic mail: junj@ee.uec.ac.jp

stabilization occurs when the configuration of N atoms satisfies a specific condition.[37] On the other hand, it has been reported that N atoms prefer to locate near the edge rather than in the basal plane of graphene, especially near zigzag edges.[38–42]

Several groups have investigated the structural stability and electronic properties of N doping near the edge of ZGNR using first-principles calculations.[15,16,38–42] It has been agreed that the formation energy increases as a function of the distance between the N atom and the edge, but it is not always understood why this should be so. In addition, questions have arisen as to the appearance of the impurity level: on one hand, it has been reported that the energy level associated with the doped N atom monotonically increases as the N atom departs from the edge,[40,41] but on the other hand, Jiang *et al.* have reported that the impurity level of the N atom appears below (above) the Fermi level when the N atom is located at odd-numbered (even-numbered) sites, respectively.[39]

In this study, we propose a mechanism for the structural stabilization of impurity atoms (N or B) located near the edge of a ZGNR based on *the charge transfer model* and propound a reasonable interpretation of the manifestation of impurity levels. We investigate the dependencies of structural stability and the electronic structure on the location of the doping site. In particular, we focus on the formation energy of the impurity atom, the impurity level, the spin-magnetic moment, and their relationships from the perspective of the charge transfer model we propose. Furthermore, we demonstrate that N- or B-doped ZGNRs have the potential to be a magnetic material with a ferromagnetic ground state.

II. CALCULATIONS

We have investigated the structural stability of an impurity atom near the edge of a ZGNR. The ZGNR had a width of seven zigzag chains of carbon atoms. Dangling bonds of C atoms at the edge were terminated by H atoms. Doping sites, where the carbon atom was substituted by an N or B atom, were distinguished by the number (1–7) of atoms that they were away from the edge (see Figure 1). We employed a supercell geometry with unit cell lengths of $a_0 = 14.8$ Å along the ribbon axis for the evaluation of the formation energy and $a_0 = 9.8$ Å for the spin-magnetic moment evaluation. Periodically arranged ribbons in the boundary condition were separated by 15 Å along the other axes, which was large enough to avoid interactions between adjacent ribbons. The structural stability of impurity atoms was evaluated on the basis of the formation energy, E_f,

$$E_f = (E_{N(B)} + \mu_C) - (E_0 + \mu_{N(B)}),   (1)$$

where $E_{N(B)}$ and E_0 are the total energies for N-doped (B-doped) and pristine ZGNR, respectively. μ_C, μ_N, and μ_B are the chemical potentials of C, N, and B, respectively. In this study, we adopted the energy per atom of pristine graphene, the N_2 molecule, or the β-rhombohedral crystal as the chemical potential for C, N, or B, respectively. A positive
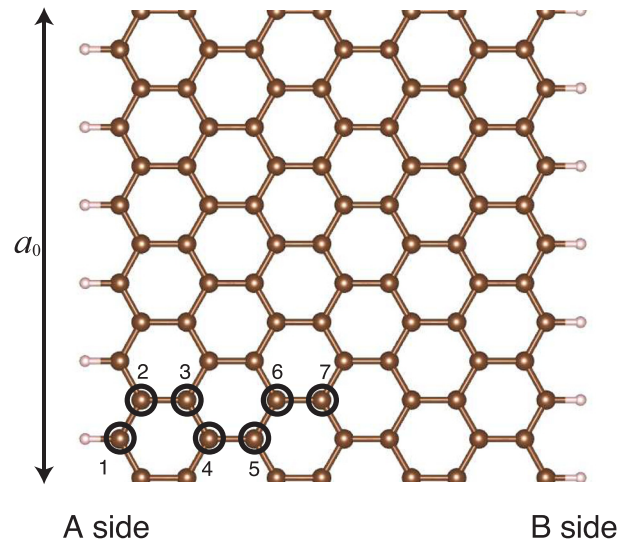

FIG. 1. Supercell of a hydrogen-passivated ZGNR with seven zigzag chains of carbon atoms, in which the unit cell length along the ribbon axis is $a_0 = 14.8$ Å. Brown and white balls indicate carbon and hydrogen atoms, respectively. The numbers 1–7 indicate doping sites. The left (right) edge is labeled the A(B) side.

(negative) valued E_f denotes that the doping reaction is endothermic (exothermic).

We performed the first-principles calculations based on the density functional theory using the Vienna *ab initio* simulation package (vasp) code.[43,44] The wave function was expanded with a plane-wave basis set with energy cutoffs of 400 eV for the formation energy calculations and 600 eV for the spin-magnetic moment calculations. The generalized gradient functional given by Perdew and Wang was utilized as the exchange-correlation functional.[45,46] The ultrasoft pseudopotentials were generated using the Vanderbilt strategy.[47] Integration over the 1D Brillouin zone (BZ) was performed using eight k-point sampling in the irreducible BZ. Structural optimization with respect to ionic positions was performed until each component of the interatomic force became less than 1.0×10^{-2} eV/Å.

III. RESULTS AND DISCUSSION

A. Dependence of the formation energy on the distance of the dopant from the zigzag edge

Figure 2 shows the dependence of the formation energy for the N- or B-doped ZGNR on the distance of the dopant from the zigzag edge. The horizontal dashed lines in Figures 2(a) and 2(b) show the formation energies in 2D graphene, which are calculated using the (7×7) supercell of graphene with one impurity atom. The difference in formation energies between ZGNR and graphene is also shown (ΔE_f, right y-axis in Figure 2). It can be seen that the formation energies for both N and B increase with the distance from the edge and converge toward the dashed lines. The tendency of the impurity atom preferring to be located near the edge agrees well with previous studies.[38–42] As shown in Figure 2, the formation energy for site 1 becomes negative, which means that the incorporation of N or B is
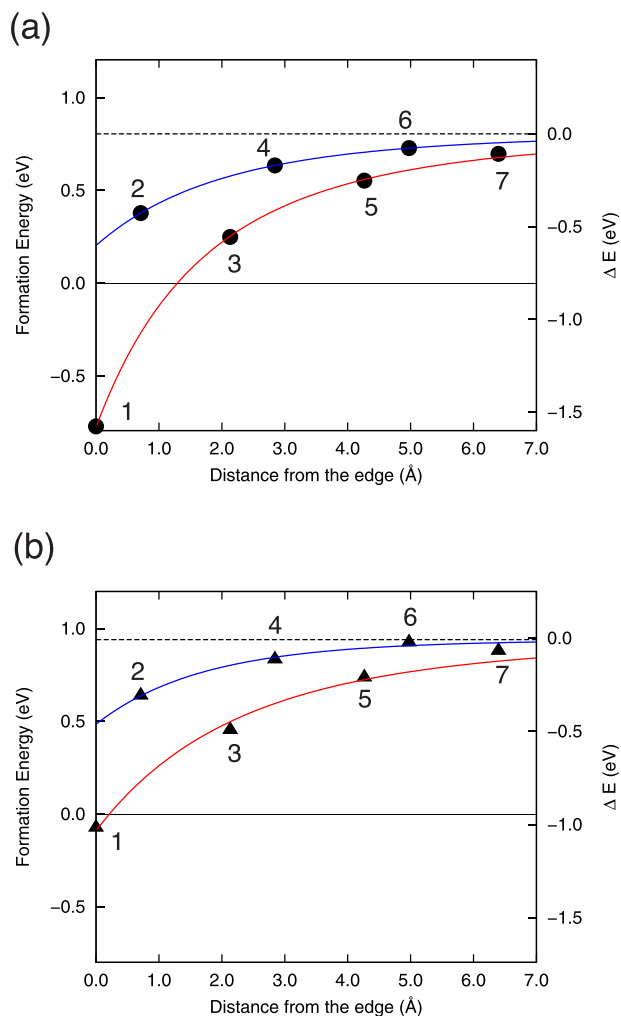
(a)

(b)

FIG. 2. Formation energies for (a) the N-doped and (b) the B-doped ZGNR. The dashed horizontal line indicates the formation energy of the N or B atom in the 2D graphene. ΔE in the right *y*-axis indicates the difference in formation energies between ZGNR and 2D graphene.

exothermic. Note that the magnitude of the change in ΔE_f for N is greater than that for B.

What has to be noted is that the increase in the formation energy with the distance from the edge is not monotonic; two independent curves arise for the odd- and even-numbered sites. Such an odd-even trend in the formation energy has also been reported in previous studies.[39,41] However, the mechanism of the site-dependent stabilization has not been clarified yet. It is important to note that the bipartite lattice like graphene has two equivalent sublattices. If the symmetry is broken by the introduction of zigzag edges, the two sublattices, the odd- and even-numbered sites, become non-equivalent to each other. Such a sublattice-dependent stabilization mechanism is discussed in Sec. III B.

B. Mechanism of the stabilization

In this section, we investigate the mechanism for doping site-dependent stabilization. It is well-known that ZGNR has localized states at the zigzag edges, and their electronic dispersion along the ribbon axis is partly flat at the Fermi

level.[6,10] The existence of these edge states is also confirmed by first-principles calculations.[11] Figure 3 shows the band structure and density of states (DOS) of pristine ZGNR as well as the partial DOS for the outermost C atom. For ZGNR with finite ribbon width, an antiferromagnetic coupling between two edges leads to the band gap opening.[7,12] Hereafter, we define the Fermi level as the center of the valence band maximum and the conduction band minimum. As shown in Figure 3, we can find two flatbands just below and above the Fermi level; these are the so-called edge states. Figure 3(d) shows a schematic energy diagram for the edge state. For the occupied state, the β-spin (α-spin) state is localized at the A (B) side of the edge, and vice versa for the unoccupied state. Note that these edge states have significant amplitude only at the odd-numbered sites.

Figures 4(a), 4(b), and 4(c) show the band structure, the total DOS, and the partial DOS of the N atom at site 1 for N-doped ZGNR, respectively. A noticeable difference from
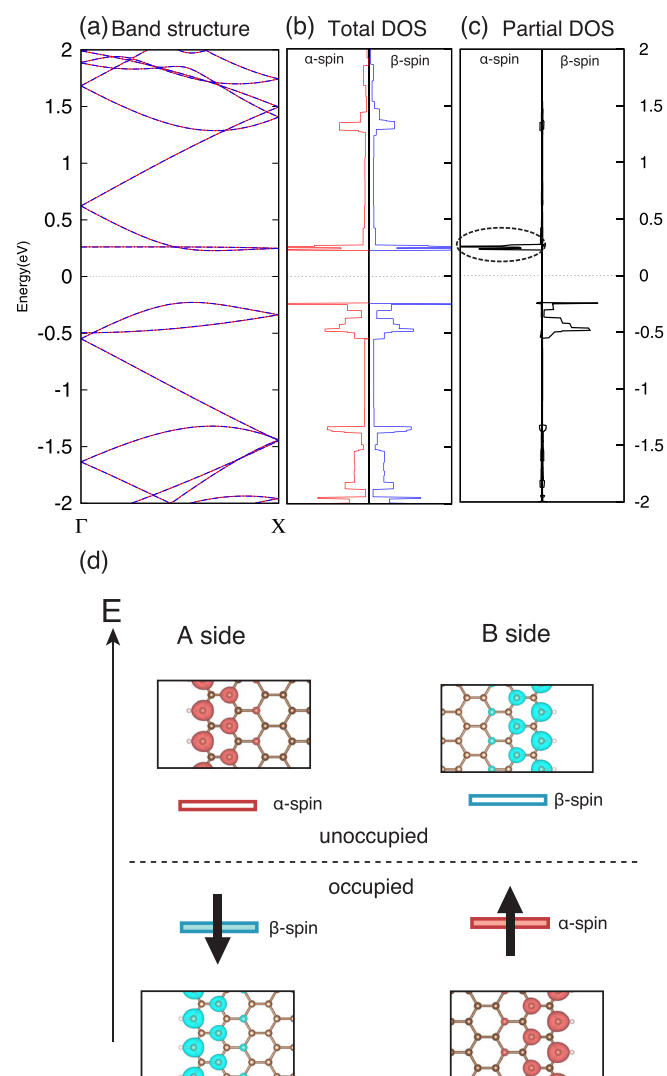

(d)

FIG. 3. Electronic structure of pristine ZGNR. (a) Band structure of ZGNR. Red and blue lines indicate α- and β-spin states, respectively. (b) Total DOS of ZGNR. (c) Partial DOS for the $2p_z$ orbital of the outermost C atom (site 1). The dashed ellipse highlights the energy level for the edge state localized at the A side for α-spin. (d) Schematic energy diagram of the edge state. The probability density for each energy level is also shown. Red and blue colors indicate α- and β-spin states, respectively.
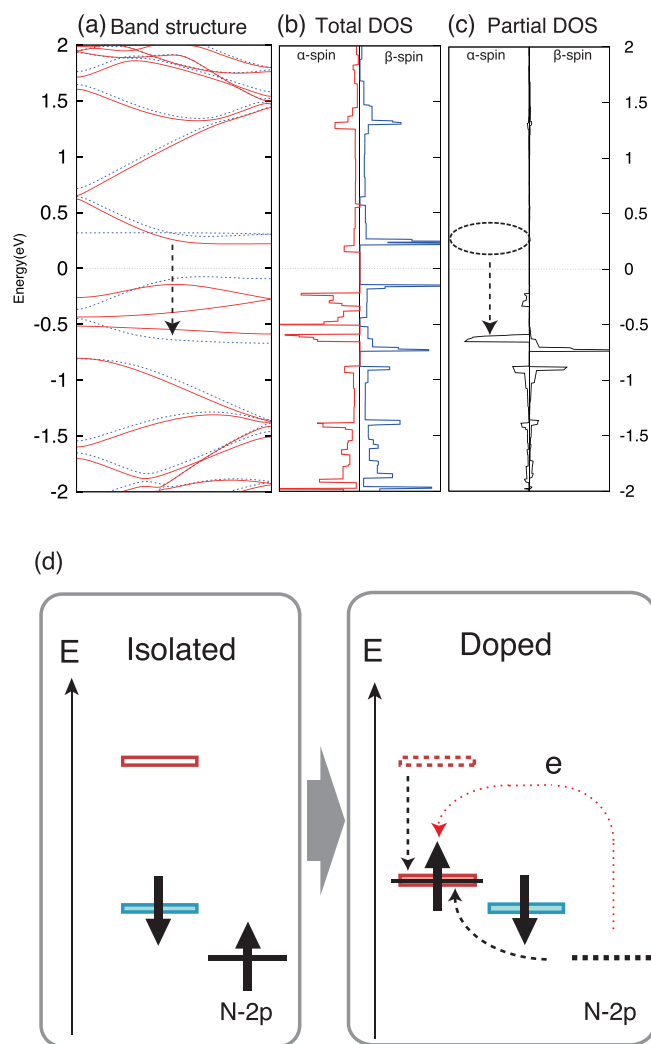
FIG. 4. Electronic structure of N-doped ZGNR (site 1). (a) Band structure of N-doped ZGNR. Red and blue lines indicate α- and β-spin states, respectively. (b) Total DOS of N-doped ZGNR. (c) Partial DOS for the $2p_z$ orbital of the N atom. (d) Schematic of the charge transfer model. The red dotted arrow shows the electron transfer associated with the doping, which causes the energy level shifts indicated by the dashed arrows.

FIG. 5. Electronic structure of N-doped ZGNR (site 2). (a) Band structure of N-doped ZGNR. Red and blue lines indicate α- and β-spin states, respectively. (b) Total DOS of N-doped ZGNR. (c) Dashed and solid lines show the partial DOS for the $2p_z$ orbital of the N atom (site 2) and that of the outermost C atom, respectively. (d) Schematic of the charge transfer model. The red dotted arrow shows the electron transfer associated with the doping, which causes the energy level shifts indicated by the dashed arrows.

the pristine ZGNR (Figure 3) is that the originally unoccupied α-spin state drops below the Fermi level and then becomes occupied, as indicated by the dashed arrows in Figure 4. A nitrogen atom at the graphitic site has five valence electrons, four of which form σ and π bonds, and the one extra electron of N results in the occupation of the empty state. Since the edge state has amplitude at odd-numbered sites, including the N atom on site 1, this state can resonate with the N-$2p_z$ orbital, which leads to the lowering of the eigenvalue. Such formation of a resonant state between the N-$2p_z$ and the edge state takes place for every odd-numbered sites. Hence, one of the valence electrons of N takes part in the edge state that is delocalized along the zigzag edge, and the N atom becomes positively charged.

For site 2, the additional electron of N also occupies the α-spin (unoccupied edge) state, and the energy of this state drops below the Fermi level as indicated by the dashed arrows in Figure 5, which is similar to the case for site 1. This is because charge transfer occurs from the N-$2p$ state to
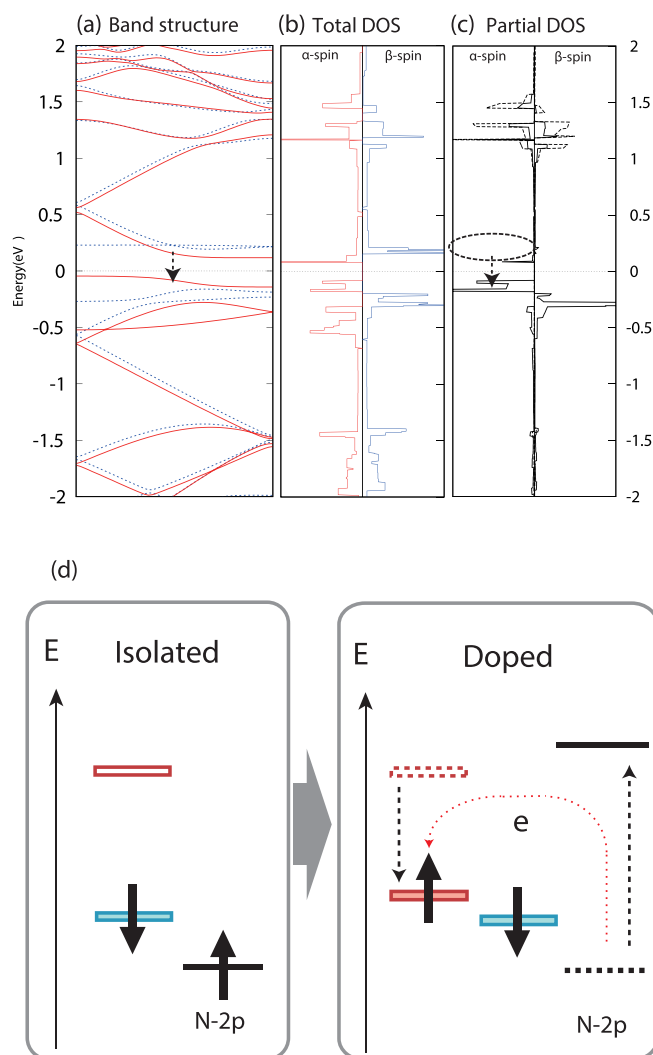
the unoccupied edge state. However, the edge state does not resonate with the N-$2p_z$ orbitals, unlike the odd-numbered case, because the edge state has no amplitude at the even-numbered doping sites. As a result, the distinct DOS for the N-$2p_z$ state appears around 1.2 eV above the Fermi level, as shown in Figure 5(c).

Although in recent years a considerable number of studies have focused on the modification of the electronic structure of graphene by N or B doping, there is room for various interpretations. For example, it was reported that the impurity level of N-doped ZGNR shifts up monotonically as the N atom departs from the edge.[40,41] Jiang *et al.* reported that the impurity level of N atoms located at odd-numbered sites appears below the Fermi level, whereas that located at even-numbered sites appears above the Fermi level.[39] On the other hand, Huang *et al.* studied the mechanism of the electronic structure modifications by N doping and proposed a screening mechanism near the doping site.[38] However, little

attention was paid to the impurity levels of N atoms at the unoccupied state for even-numbered site doping. In our study, it has been revealed that the N-$2p_z$ state appears in the occupied (unoccupied) state for doping at odd- (even-) numbered sites. Such a specific electronic structure can be explained by the charge transfer between N-$2p$ and the edge state, as we have described. Furthermore, the charge transfer mechanism can also explain the characteristics of the formation energy (seen in Figure 2), as discussed below.

Here, we focus on the correlation between the stability and the lowering of the one-electron energy of the edge state induced by the charge transfer. Figure 6 shows the relationship between the formation energy and the depth of the one-electron orbital energy of the edge state. The depth of the one-electron orbital energy of the edge state is measured from the Fermi level, as defined in the this section. We can definitely confirm the positive correlation between them in Figure 6, which suggests that the one-electron orbital energy of the edge state dominates the stability of the N-doped graphene. The extra electron from the N atom occupies the edge state, resulting in an attractive electrostatic interaction between the positively charged N cation and the electron delocalized at the zigzag edge. This attractive interaction energy decreases as the N atom departs from the edge. This is the reason why the formation energy increases with the distance of the N atom from the edge. In addition, the occupied edge state (α-spin), which is originally unoccupied, resonates with the N-$2p_z$ orbital for odd-site doping, but this is not the case for even-site doping. As a result, the one-electron orbital energy of the edge state for odd-site doping is systematically lower than that for even-site doping. Therefore, two independent curves of the formation energy arise for the odd- and even-numbered sites, respectively. Such an explicit correlation between the formation energy and the depth of the one-electron orbital energy of the edge state demonstrates that the electronic structure of the N-doped graphene is well-described by the charge transfer between the edge state and the N-$2p_z$ orbital.

The attractive interaction between the N atom and the edge becomes negligible if the N atom is situated sufficiently away from the edge. In such a case, no exchange of electrons between the N atom and the edge occurs. Instead, the extra electron released from N occupies the anti-bonding π^*-band of graphene. Hence, the Fermi level shifts up into the conduction band, resulting in a metal-like system, as schematically shown in Figure 7. Indeed, such a rigid band shift has been confirmed for N doping in the basal plane of graphene.[37] In this case, the system gains kinetic energy because of the large energy dispersion of the π^*-band.

For B doping, on the other hand, an additional hole is provided by the B atom instead of an extra electron provided by the N atom. The mechanism of the stabilization for B doping is attributed to the same mechanism as for N doping; the hole derived from the B atom transfers to the occupied edge state, as shown in Figures S1 and S2 in the supplementary material. Note that there is a difference in the absolute values of the formation energy; the degree of the change in ΔE_f for N is greater than that for B, as shown in Figure 2. The charge transfer model can offer an explanation for such an overall trend in ΔE_f as follows. For N doping, the extra electron of N becomes delocalized at the edge owing to the charge (electron) transfer. For B doping, on the other hand, the electron of the originally occupied edge state becomes localized at the B atom site due to the charge (hole) transfer from the B-$2p$ orbital to the edge state, which leads to a repulsive Coulomb energy.

Finally, we address the stability of the hydrogenation of N at the zigzag edge. In this study, the N(B) atom located at site 1 is terminated by a H atom, as improbable as it may sound. Indeed, the N atom of a pyridine molecule is rarely accompanied by an H atom, since the N atom of pyridine has a stable lone pair of electrons. However, the N atom at the zigzag edge prefers to be hydrogenated, maintaining the planar C-N-C structure. Figure 8 shows the formation energy of the N-H bond at the zigzag edge of ZGNR, $\Delta E_\mathrm{N-H} = E_\mathrm{N-H} - (E_\mathrm{N} + \mu_\mathrm{H})$, where $E_\mathrm{N-H}$, E_N, and μ_H are the total energies of fully hydrogenated ZGNR, ZGNR with pyridinic-N, and the chemical potential of hydrogen, respectively. The
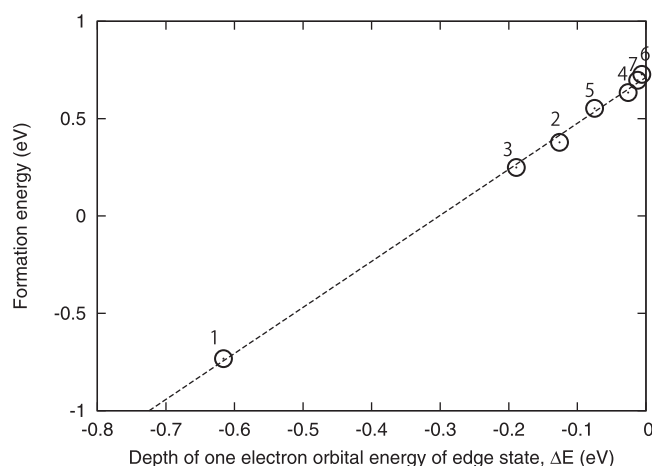

FIG. 6. Correlation between the formation energy and the depth of the one-electron orbital energy of the edge state. The numbers above the points correspond to the N doping sites. The dashed line indicates the result of a linear fit.
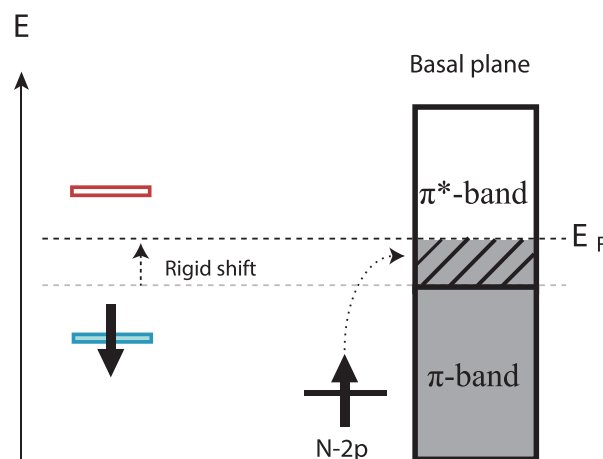

FIG. 7. Schematic energy diagram of N doping in the basal plane of graphene. The dashed arrow indicates the change in the energy level associated with the electron transfer. The dotted arrow shows the electron transfer.
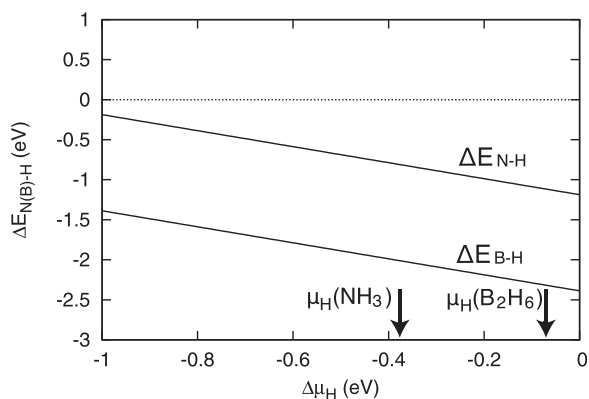
FIG. 8. Formation energy of the N-H (B-H) bond at the edge of ZGNR as a function of the chemical potential of H. The chemical potential of the hydrogen molecule is defined as zero. A negative sign of $\Delta E_{N(B)-H}$ means that the N(B) atom at the edge prefers to be hydrogenated.

formation energies for the B-H bond are also shown. As clearly shown in this figure, the hydrogenation of N(B) becomes favorable within the normal range of μ_H. Such formation of a stable N-H bond corroborates the charge transfer model; if the extra electron (hole) transfers to the edge state, one of the electrons of N(B) contributes to the formation of the covalent bonding between N(B) and H and then the π-conjugated network near the edge is preserved, even with N(B) doping.

C. Magnetic properties

Pristine ZGNR with a finite width has an antiferromagnetic spin configuration in its ground state.[7,12,14] On the other hand, in this study, the N-doped (B-doped) ZGNR is predicted to have a ferromagnetic ground state, when the N(B) atom dopant is situated near the edge. Figure 9 shows the energy difference between ferromagnetic and antiferromagnetic ground states, $\Delta E_{spin} = E_{FM} - E_{AFM}$, where E_{AM} and E_{AFM} are the total energies for the ferromagnetic and antiferromagnetic states, respectively. The ground state of this system switches between ferromagnetic and antiferromagnetic, as shown in Figure 9. Such a tendency in ΔE_{spin} can be
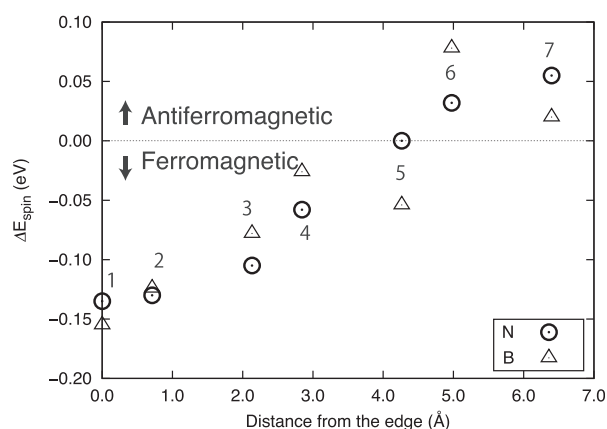

FIG. 9. Energy differences between antiferromagnetic and ferromagnetic states as a function of the distance of the dopant from the edge. Circles and triangles correspond to the N and B dopings, respectively. The numbers in the plots correspond to the doping sites.

explained by the charge transfer model. For the N-doped (B-doped) ZGNR, an extra electron (hole) transfers to the unoccupied (occupied) edge state, resulting in the compensation (disappearance) of the spin-magnetic moment at one side of the edges. Since the spin-magnetic moment at the other side remains unchanged, the total spin-magnetic moment of the system becomes non-zero. On the other hand, when the N(B) atom is doped sufficiently away from the edge, the antiferromagnetic configuration becomes the ground state, since the edge states for both sides are hardly affected by the doping. What has to be noticed here is that $|\Delta E_{spin}|$ for site 1 is 0.135 eV, which is much larger than the thermal energy at room temperature. In light of the energetic stability of site 1, N(B) doping appears to be a more practical and realistic way of fabricating magnetic carbon materials compared with the fabrication of dihydrogenated[13] and BN-terminated[14] ZGNRs.

IV. CONCLUSIONS

We have studied the dependence of the structural stability of N-doped (B-doped) ZGNR on the distance of the N(B) atom from the zigzag edge. The formation energy increases as a function of the distance of the dopant atom from the edge, and two independent curves arise for odd- and even-numbered sites. Such an energetic dependence is successfully explained by the charge transfer model; when the N(B) atom dopant is located near the edge, the extra electron (hole) of the N(B) atom transfers to the edge state, resulting in the occupation (vacation) of the originally unoccupied (occupied) edge state. Since the edge state has amplitude only at odd-numbered sites, only the N-$2p_z$ orbital at odd-numbered sites can resonate with the edge state; thus, the eigenvalue of the edge state for odd-numbered-site doping becomes lower than that for even-numbered-site doping. The gain in the electrostatic energy between the N cation (B anion) and the extra electron (hole) delocalized at the edge decreases with increasing distance of the N(B) atom from the edge, which leads to the trend of increasing formation energy. On the other hand, when the N(B) atom dopant is located sufficiently away from the edge, the extra electron (hole) is no longer transferred to the edge, but occupies the π^*-band (π-band), which results in a kinetic energy gain because of the large energy dispersion of the π^*-band (π-band). The controversy surrounding the impurity level for doped graphene is settled owing to the charge transfer model. Such an electron (hole) transfer leads to compensation (disappearance) of the local spin-magnetic moment at one side of the edges of ZGNR, while the local spin-magnetic moment at the other side remains unchanged. As a result, the N- or B-doped ZGNR becomes ferromagnetic. Since recent experimental progress makes it possible to fabricate well-controlled ZGNR,[48–51] doped-ZGNRs must be highlighted as promising candidates for new types of lightweight magnetic materials.

SUPPLEMENTARY MATERIAL

See supplementary material for the band structures of the N-doped ZGNRs.

[1] K. Novoselov, A. Geim, S. Morozov, D. Jiang, Y. Zhang, S. Dubonos, I. Grigorieva, and A. Firsov, Science **306**, 666 (2004).

[2] K. I. Bolotin, K. J. Sikes, Z. Jiang, M. Klima, G. Fudenberg, J. Hone, P. Kim, and H. L. Stormer, Solid State Commun. **146**, 351 (2008).

[3] K. Saito, J. Nakamura, and A. Natori, Phys. Rev. B **76**, 115409 (2007).

[4] A. A. Balandin, S. Ghosh, W. Bao, I. Calizo, D. Teweldebrhan, F. Miao, and C. N. Lau, Nano Lett. **8**, 902 (2008).

[5] S. Ghosh, I. Calizo, D. Teweldebrhan, E. P. Pokatilov, D. L. Nika, A. A. Balandin, W. Bao, F. Miao, and C. N. Lau, Appl. Phys. Lett. **92**, 151911 (2008).

[6] K. Nakada, M. Fujita, G. Dresselhaus, and M. S. Dresselhaus, Phys. Rev. B **54**, 17954 (1996).

[7] Y.-W. Son, M. L. Cohen, and S. G. Louie, Phys. Rev. Lett. **97**, 216803 (2006).

[8] D. Klein, Chem. Phys. Lett. **217**, 261 (1994).

[9] D. Gunlycke, D. A. Areshkin, J. Li, J. W. Mintmire, and C. T. White, Nano Lett. **7**, 3608 (2007).

[10] M. Fujita, K. Wakabayashi, K. Nakada, and K. Kusakabe, J. Phys. Soc. Jpn. **65**, 1920 (1996).

[11] Y. Miyamoto, K. Nakada, and M. Fujita, Phys. Rev. B **59**, 9858 (1999).

[12] G. Lee and K. Cho, Phys. Rev. B **79**, 165440 (2009).

[13] K. Kusakabe and M. Maruyama, Phys. Rev. B **67**, 092406 (2003).

[14] J. Nakamura, T. Nitta, and A. Natori, Phys. Rev. B **72**, 205429 (2005).

[15] Y. Li, Z. Zhou, P. Shen, and Z. Chen, ACS Nano **3**, 1952 (2009).

[16] X. H. Zheng, X. L. Wang, T. A. Abtew, and Z. Zeng, J. Phys. Chem. C **114**, 4190 (2010).

[17] T. Ohta, A. Bostwick, T. Seyller, K. Horn, and E. Rotenberg, Science **313**, 951 (2006).

[18] R. Lv and M. Terrones, Mater. Lett. **78**, 209 (2012).

[19] O. Hod, V. Barone, J. E. Peralta, and G. E. Scuseria, Nano Lett. **7**, 2295 (2007).

[20] D. Gunlycke, J. Li, J. W. Mintmire, and C. T. White, Appl. Phys. Lett. **91**, 112108 (2007).

[21] X. Wang, X. Li, L. Zhang, Y. Yoon, P. K. Weber, H. Wang, J. Guo, and H. Dai, Science **324**, 768 (2009).

[22] D. Wei, Y. Liu, Y. Wang, H. Zhang, L. Huang, and G. Yu, Nano Lett. **9**, 1752 (2009).

[23] B. Guo, Q. Liu, E. Chen, H. Zhu, L. Fang, and J. R. Gong, Nano Lett. **10**, 4975 (2010).

[24] Y.-C. Lin, C.-Y. Lin, and P.-W. Chiu, Appl. Phys. Lett. **96**, 133110 (2010).

[25] L. Zhao, R. He, K. T. Rim, T. Schiros, K. S. Kim, H. Zhou, C. Gutiérrez, S. P. Chockalingam, C. J. Arguello, L. Pálová, D. Nordlund, M. S. Hybertsen, D. R. Reichman, T. F. Heinz, P. Kim, A. Pinczuk, G. W. Flynn, and A. N. Pasupathy, Science **333**, 999 (2011).

[26] L. Zhao, M. Levendorf, S. Goncher, T. Schiros, L. Pálová, A. Zabet-Khosousi, K. T. Rim, C. Gutiérrez, D. Nordlund, C. Jaye, M. Hybertsen, D. Reichman, G. W. Flynn, J. Park, and A. N. Pasupathy, Nano Lett. **13**, 4659 (2013).

[27] Y.-B. Tang, L.-C. Yin, Y. Yang, X.-H. Bo, Y.-L. Cao, H.-E. Wang, W.-J. Zhang, I. Bello, S.-T. Lee, H.-M. Cheng, and C.-S. Lee, ACS Nano **6**, 1970 (2012).

[28] R. J. Koch, M. Weser, W. Zhao, F. Viñes, K. Gotterbarm, S. M. Kozlov, O. Höfert, M. Ostler, C. Papp, J. Gebhardt, H.-P. Steinrück, A. Görling, and T. Seyller, Phys. Rev. B **86**, 075401 (2012).

[29] H. Niwa, K. Horiba, Y. Harada, M. Oshima, T. Ikeda, K. Terakura, J. Ozaki, and S. Miyata, J. Power Sources **187**, 93 (2009).

[30] L. Qu, Y. Liu, J.-B. Baek, and L. Dai, ACS Nano **4**, 1321 (2010).

[31] L. Zhang and Z. Xia, J. Phys. Chem. C **115**, 11170 (2011).

[32] D. Usachov, O. Vilkov, A. Grüneis, D. Haberer, A. Fedorov, V. K. Adamchuk, A. B. Preobrajenski, P. Dudin, A. Barinov, M. Oehzelt, C. Laubschat, and D. V. Vyalikh, Nano Lett. **11**, 5401 (2011).

[33] H. J. Xiang, B. Huang, Z. Y. Li, S.-H. Wei, J. L. Yang, and X. G. Gong, Phys. Rev. X **2**, 011003 (2012).

[34] Z. Hou, X. Wang, T. Ikeda, K. Terakura, M. Oshima, M. Kakimoto, and S. Miyata, Phys. Rev. B **85**, 165439 (2012).

[35] Z. Hou, X. Wang, T. Ikeda, K. Terakura, M. Oshima, and M. Kakimoto, Phys. Rev. B **87**, 165401 (2013).

[36] T. Kondo, S. Casolo, T. Suzuki, T. Shikano, M. Sakurai, Y. Harada, M. Saito, M. Oshima, M. I. Trioni, G. F. Tantardini, and J. Nakamura, Phys. Rev. B **86**, 035436 (2012).

[37] T. Umeki, A. Akaishi, A. Ichikawa, and J. Nakamura, J. Phys. Chem. C **119**, 6288 (2015).

[38] S.-F. Huang, K. Terakura, T. Ozaki, T. Ikeda, M. Boero, M. Oshima, J. Ozaki, and S. Miyata, Phys. Rev. B **80**, 235410 (2009).

[39] J. Jiang, J. Turnbull, W. Lu, P. Boguslawski, and J. Bernholc, J. Chem. Phys. **136**, 014702 (2012).

[40] S. Yu, W. Zheng, Q. Wen, and Q. Jiang, Carbon **46**, 537 (2008).

[41] E. Cruz-Silva, Z. M. Barnett, B. G. Sumpter, and V. Meunier, Phys. Rev. B **83**, 155445 (2011).

[42] M. Li, L. Zhang, Q. Xu, J. Niu, and Z. Xia, J. Catal. **314**, 66 (2014).

[43] G. Kresse and J. Furthmüller, Comput. Mater. Sci. **6**, 15 (1996).

[44] G. Kresse and J. Furthmüller, Phys. Rev. B **54**, 11169 (1996).

[45] J. P. Perdew, J. A. Chevary, S. H. Vosko, K. A. Jackson, M. R. Pederson, D. J. Singh, and C. Fiolhais, Phys. Rev. B **46**, 6671 (1992).

[46] J. P. Perdew, J. A. Chevary, S. H. Vosko, K. A. Jackson, M. R. Pederson, D. J. Singh, and C. Fiolhais, Phys. Rev. B **48**, 4978 (1993).

[47] D. Vanderbilt, Phys. Rev. B **41**, 7892 (1990).

[48] J. Cai, P. Ruffieux, R. Jaafar, M. Bieri, T. Braun, S. Blankenburg, M. Muoth, A. P. Seitsonen, M. Saleh, X. Feng, K. Mullen, and R. Fasel, Nature **466**, 470 (2010).

[49] A. G. Cano-Márquez, F. J. Rodríguez-Macías, J. Campos-Delgado, C. G. Espinosa-González, F. Tristán-López, D. Ramírez-González, D. A. Cullen, D. J. Smith, M. Terrones, and Y. I. Vega-Cantú, Nano Lett. **9**, 1527 (2009).

[50] G. Z. Magda, X. Jin, I. Hagymasi, P. Vancso, Z. Osvath, P. Nemes-Incze, C. Hwang, L. P. Biro, and L. Tapaszto, Nature **514**, 608 (2014).

[51] M. Terrones, A. R. Botello-Méndez, J. Campos-Delgado, F. López-Urías, Y. I. Vega-Cant, F. J. Rodríguez-Macías, A. L. Elías, E. Muñoz-Sandoval, A. G. Cano-Márquez, J.-C. Charlier, and H. Terrones, Nano Today **5**, 351 (2010).